*Trends in Immunotherapy* 2024, 8(2), 8937.
https://doi.org/10.24294/ti.v8.i2.8937

Article

# Cancer new treatment series: Comparison immune changes of HCC by scRNA-Seq following HELC treatment one case study

**Baofa Yu[1,2,3,4,5,*], Feng Gao[1], Peng Jing[1], Peicheng Zhang[1], Jian Zhang[2], Guoqin Zheng[1]**

[1] TaiMeiBaofa Cancer Hospital, Dongping 271500, Shandong Province, China
[2] Jinan Baofa Cancer Hospital, Jinan 250000, Shandong Province, China
[3] Beijing Baofa Cancer Hospital, Beijing 100010, China
[4] Immune Oncology Systems, Inc, San Diego, CA 92102, USA
[5] South China of Hospital, Shenzhen University, Shenzhen 518055, Guangdong Province, China
*** Corresponding author:** Baofa Yu, bfyuchina@126.com

**CITATION**

Yu B, Gao F, Jing P, et al. Cancer new treatment series: Comparison immune changes of HCC by scRNA-Seq following HELC treatment one case study. Trends in Immunotherapy. 2024; 8(2): 8937. https://doi.org/10.24294/ti.v8.i2.8937

**ARTICLE INFO**

Received: 2 September 2024
Accepted: 11 September 2024
Available online: 21 October 2024



**Abstract:** Immunotherapy has emerged as a novel treatment strategy for many types of cancers, among them, liver cancer. The major advances and achievements in recent years is the use of programmed death-1 (PD-1) blockers for cancer treatment. Since patients' immune systems are already weak following concurrent surgery plus chemo or radiotherapy, it is necessary to restore and awake their immune cells to maximize the effect for immune therapy. Methods: Liver cancers were treated twice with hapten enhanced local chemotherapy (HELC) like tumor lysates vaccine and following PD-1. Single-cell RNA sequencing (scRNA-seq) was used to analyze the changes of immune responses prior and after treatments. Results: We observed upregulation of cytotoxicity-related genes of CD8 effector T cells and NK cells in untreated tumor; Both Bmem and Naive B cells in untreated tumor showed a significant increase in MHC II signaling pathway-related genes, while MHC I-related genes was upregulated in plasma cells. Significant tumor size shrinkage was observed in both treated and untreated tumors following the HELC+PD-1 therapy. Conclusions: This study provides new biological insights into the abscopal effect at the single-cell level related to the composition of T and B cells in untreated liver cancers before and after major primary tumors treated by HELC. Our data showed that intra-tumor HELC can kill tumor cells and induced immune activity, which is likely vital in modifying tumor associate antigens (TAAs) into neo TAAs. It induces immune response just like vaccine can wake up immune cells and therefore increasing the efficacy of PD1 therapy.

**Keywords:** immunotherapy; Programmed Death-1 (PD-1) blockers; single-cell RNA sequencing (scRNA-seq); MHC signaling pathway-related genes; liver tumor treated by hapten enhanced local chemotherapy

## 1. Introduction

Incidence of liver cancer (tumors) has progressively declined in the United States and increasing in China [1]. Multifocal tumors that develop from primary intrahepatic metastasis (IM) or multicentric progression (MO) are a distinct feature of hepatocellular carcinoma (HCC) [2]. Only a few of multifocal tumor of HCC were under the control of immune-surveillance, while others evaded the immune system through multiple mechanisms that led to poor prognosis [2]. Local treatment and new treatment options are necessary to treat liver primary cancers [3]. Immunotherapy has emerged as a novel treatment strategy for HCC include multifocal tumor HCCs. This immunotherapy has also succeeded in HCCs [4]. In clinical practice, most patients receive standard of care with concurrent chemo or radiation therapy (CCRT). As a

result, patient's immune system had been damaged to a lower level, as result, T cells are in weak to sick (WtoS) condition, any immunotherapy cannot achieve the expected effect. Recent advancement is using hapten combining with chemotherapeutic drugs, has been successfully injected into local tumor body for treatment of HCC [5].

It is key to wake up the immune cells and restore the specificity of identifying tumor cells during treatment. Ultra-minimum incision personalized intra-tumor chemoimmunotherapy (UMIPIC) is new tool for treating cancer [6]. UMIPIC is a method of chemo drug kill tumor and can further trigger the release of damage-associated molecular patterns (DAMPs) and antigens from dying tumor cells, which is modified by hapten to be neo TAAs within tumor to activate the innate immune response, it likes the tumor lysate vaccine to induce immune response, especially whole cancer cells or cancer cell lysates, it is a very promising approach associated with T cell immunity [7–9]. The progress of single-cell RNA sequencing (scRNA-seq) allows scientists to explore the genetic and functional heterogeneity of complexity at single cellular level [10]. However, the current single-cell studies of HCC mostly focus on the tumor microenvironment (TME) [11] and is still lack of comparative studies on the single-cell level on HCC with immune reaction-related abscopal effect between untreated tumors and treated tumor prior and post hapten enhanced UMIPIC.

1.3 This study provides new biological insight at the single cell level with multiple cell types include myeloid cells, stromal cells, T cells, plasma cells, B cells, platelets, erythrocytes and epithelial cells from untreated tumors (**Figures 1a** and **2a**) to investigate if immune cells were awakened to be ready for cancer immunotherapy like PD-1 or PD-L1 [12–14].

## 2 Materials and methods

### Clinical parameters and sample collection

Patient was a 63 years old female with HCC. Additional exclusion criteria include: display any of the following conditions: 1, Exhibit poor karnofsky performance status (KPS) (≤40%); 2, Present with a high serum bilirubin >3 mg/dL (51.3 μmol/L); 3, Has any nutritional disorder(s); or 4, has renal failure [serum creatinine >2 mg/dL (176.8 μmol/L)].

The patient presented with a big size tumor mass of 13 cm × 8 cm and multiple small tumor mass in same area. Her KPS score is 85, clinical stages IIIB (T3N0M0) according to the American NCI TNM stage system. No treatment prior enrolling to this study. **Figure 1** shows the distribution of these tumors (**Figure 1**). The patient with high abnormal prothrombin (AP) 19,184 ng/mL, Alpha-fetoproteins (AFP) was not detected (AFP ≤ 20 ng/mL). Pathologic diagnose at Shandong Province General Hospital was hepatocellular carcinoma (HCC). Circulating tumor cells (CTC) was tested with blood before enrolling [15]. Informed consent was obtained from patient. This study was approved by the Ethics Committee Board of Shandong Baofa Cancer Institute (TMBF 0010, 2015). This study was conducted in accordance with relevant guidelines and regulations. UMIPIC therapy is by injecting of a combination dosage of the following: 10 mL total of 1.00 mg/mL Adriamycin (Adr), 0.80 mg/mL of cytarabine (Ara-C), 20.0 mg/mL of $H_2O_2$ and 144 mg/mL of penicillin as hapten into the major HCC mass.

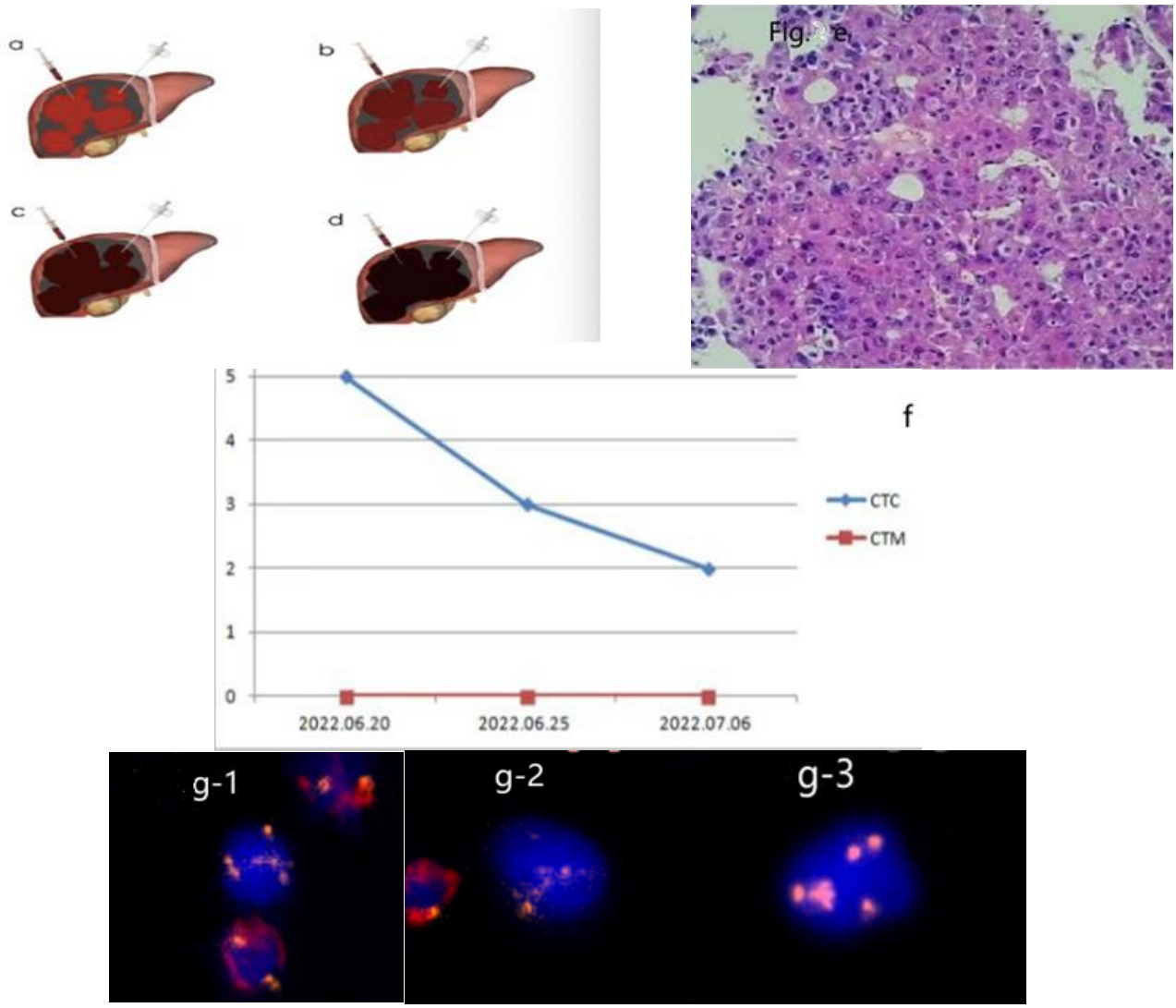


**Figure 1.** Biopsy fresh tumor tissue for scRNA-seq and syringe was took for intratumoral inject to tumor with chemotherapy drug plus hapten.

a: After left needle of biopsy was took under CT guiding for fresh tumor tissue and scRNA-seq asuntreated tissue before any therapy, the right syringe began the injection of chemotherapy drug plus hapten by CT guiding.

b: One week later, left needle of biopsy was took again under CT guiding for fresh tumor tissue and scRNA-seq as untreated tumor tissue before the right syringe began to inject of chemotherapy drugs plus hapten again to the primary major tumor near the untreated tumor for second injection by CT guiding.

c: Two week later from first treatment, left needle was injected under CT guiding for biopsy in order to check the tumor cell activity and right syringe started to inject to any tumor in the scope of huge big tumor area with chemotherapy drug plus hapten.

d: At three weeks, left needle was injected under CT guiding for biopsy again in order to check the tumor cell activity, right syringe was begun to inject of to any tumor in the scope of huge big tumor area with chemotherapy drug plus hapten by CT guiding.

e: Pathology diagnosis confirm the diagnosis is hepatocellular carcinoma.

f: CTC (ciculation tumor cell) was detected before treatment and one week later CTC decreased from 5/3 mL to 3 mL, and two week later CTC decreased to 2 mL; Circulating tumor vascular endothelial Cells (CTEC) was 0/mL for all time.

g: Photo is the CTCS: CD45, CD31, g1 is CTC before treatment, g2 and g3 is CTC after treatment; Their CEP8 chromosome is heteroploid with DAPI+.

- Subtraction enrichment (SE):

This study has made significant improvement on SE prototype protocol as it was previously published [16]. Experiments were performed according to the manufacture's instruction (Cytelligen, San Diego, CA, USA). Briefly, 6 mL of blood were collected into a tube containing ACD anti-coagulant (Becton Dickinson, Franklin Lakes, NJ, USA). Sediment blood cells were gently mixed with 3.5 mL of CTC buffer, followed by loading on the non-hematopoietic cell separation matrix in a 50 mL tube followed by subsequent centrifugation at 450 × g for 5 min. Solutions free of magnetic beads were collected into a 15 mL tube, followed by adding CTC buffer to a final volume of 14 mL. Samples were spun again at 500 × g for 4 min at room temperature. Supernatants were aspirated down to 50 μL. Sediment cells in 50 μL were gently re-suspended and subject to following preparation: primary tumor cell culture, viability check, immunofluorescence staining, or drying monolayer of cells mixed with the special fixative on the Cytelligen coated and formatted CTC slides for subsequent iFISH analyses.

- Viability examination of the tumor cells enriched from blood

About 80 to 100 of SK-BR-3 breast cancer cell-line cells were spiked into 6 mL of blood, followed by subtraction enrichment. Enriched tumor cells were incubated with AF488 labeled anti-HER2 Ab for 20 min at room temperature in dark. After incubation, cells were centrifuged at 950 × g for 4 min. Sediment cells were re-suspended with 100 μL PBS, and incubated with 10 μL of 7-aminoactionomycin D (7-AAD, 5 μg/mL) (Life Technologies, Carlsbad, CA, USA), at room temperature for 10 minutes, followed by 5 μL of nucleus staining dye Hoechst 33,342 (0.5 mg/mL, Thermo Fisher Scientific, Skokie, IL, USA) for additional 15 min at room temperature in dark. Cells were washed twice with PBS, followed by microscopic analysis. Necrotic cells nuclear were stained red with 7-AAD [17].

- Single-cell RNA sequencing (scRNA-Seg)

We followed Singleron GEXSCOPE$^{R}$ operating manuals and GEXSCOPE$^{R}$ microfluidic chip was used to capture the single cell suspension with a concentration of 1–3 × $10^5$ cells/mL. One magnetic bead paired with one cell in each micro well. Each magnetic bead has a unique cell label. So that multiple molecular labels [unique molecular identifier (UMI)] can capture RNA. When RNA was released from the captured cells, it binds to the magnetic bead. The magnetic beads were then collected into a 1.5 mL Eppendorf tube for reverse transcription reaction to generate cDNA (GEXSCOPE$^{R}$ Single-Cell RNA Library Kit was used for cDNA synthesis in single cells Singleron Biotechnologies, Nanjing, China) (**Figure 1f**). After cDNA was synthesized and PCR amplification followed on a Qubit (Thermo, Waltham, MA, USA) for cDNA quantification. Fragment Analyzer was used to determine the cDNA fragment size. After series of steps, including fragmentation, adapter ligation, purification, PCR amplification, size selection, and quality control (QC), the libraries were constructed (**Figure 1g**), and sequenced with 150 base pairs (bp) paired end reads

on IlluminaHiSeq X platform.

- Data processing and analysis

The original gene expression matrix data were generated using the CeleScope$^{R}$ (https://github.com/singleron-RD/CeleScope) software. Scanpy v1.8.2. was used for quality control, dimensionality reduction, and clustering analysis under Python 3.7. To remove batch effect, Harmony v1.0 [18,19] was used for re-clustering non-malignant immune cell types.

The InferCNV (copy number variation) package was used to detect the CNAs in malignant cells. Mononuclear phagocytes (MPs) were considered as non-malignant cells and used as baselines to estimate the CNAs of malignant cells. Given the knowledge that myeloid cells would harbor strong CNAs on chromosome 6, CNA loss on chromosome 6 from the cells of interest was not counted for malignant cell assessment [20].

Gene set scoring was performed by using the R package UCell v 1.1.0 [21].

Cell-cell interaction (CCI) was predicted based on known ligand–receptor pairs by Cellphone DB v2.1.0 [22].

## 3. Results

### 3.1. Clinical course for patient

The biopsy sample of tumor was confirmed by pathology as hepatocellular carcinoma, HCC (**Figures 1a** and **2a**). CTC were detected before and after treatment with a decreasing trend (CTC numbers decreased from 5/3 mL before treatment to 3/3 mL one week after treatment, 2/3 mL after two weeks treatment (**Figure 2f,g**). CT scan and color ultrasonic imaging showed tumor mass size was stable. The abnormal prothrombin level was observed as greatly decreased (19,184 ng/mL) and increased to 32,048 ng/mL 102 days after the first test of abnormal prothrombin and alpha-fetoproteins (AFP). This is probably due to that abnormal prothrombin was released into the blood circulation from the dead tumor cells followed intra-tumoral injection with chemotherapeutic drugs.

Patient felt better than before treatment. The itching problem didn’t change probably due to the level of abnormal prothrombin (AP) was higher. AP was a diagnostic value for AFP-negative hepatocellular carcinoma, and its level may reflect the degree of natural tumor progression. After 13 month follow up, this patient had returned to normal living condition and improved quality of health.

Abnormally high prothrombin.

In our results, KEGG pathway enrichment analysis of differential genes in tumor cells before and after treatment found that complement. The expression of prothrombin coding gene F2 was up-regulated. During protein modification, it is involved in coagulationY-glutamyl carboxylase coding gene GGCX and vitamin K epoxide reductase complex 1 modified by prohemase. The expression of the code gene VKORC was upregulated, as was the expression of the gene set associated with vitamin K metabolism, but clinical abnormal prothrombin remains high, presumably to be verified at the genomic level. It is due to the genetic changes of related enzymes, resulting in that although the gene expression is up-regulated, it cannot play a normal function and cannot form a normal enzyme (**Figure 2**).

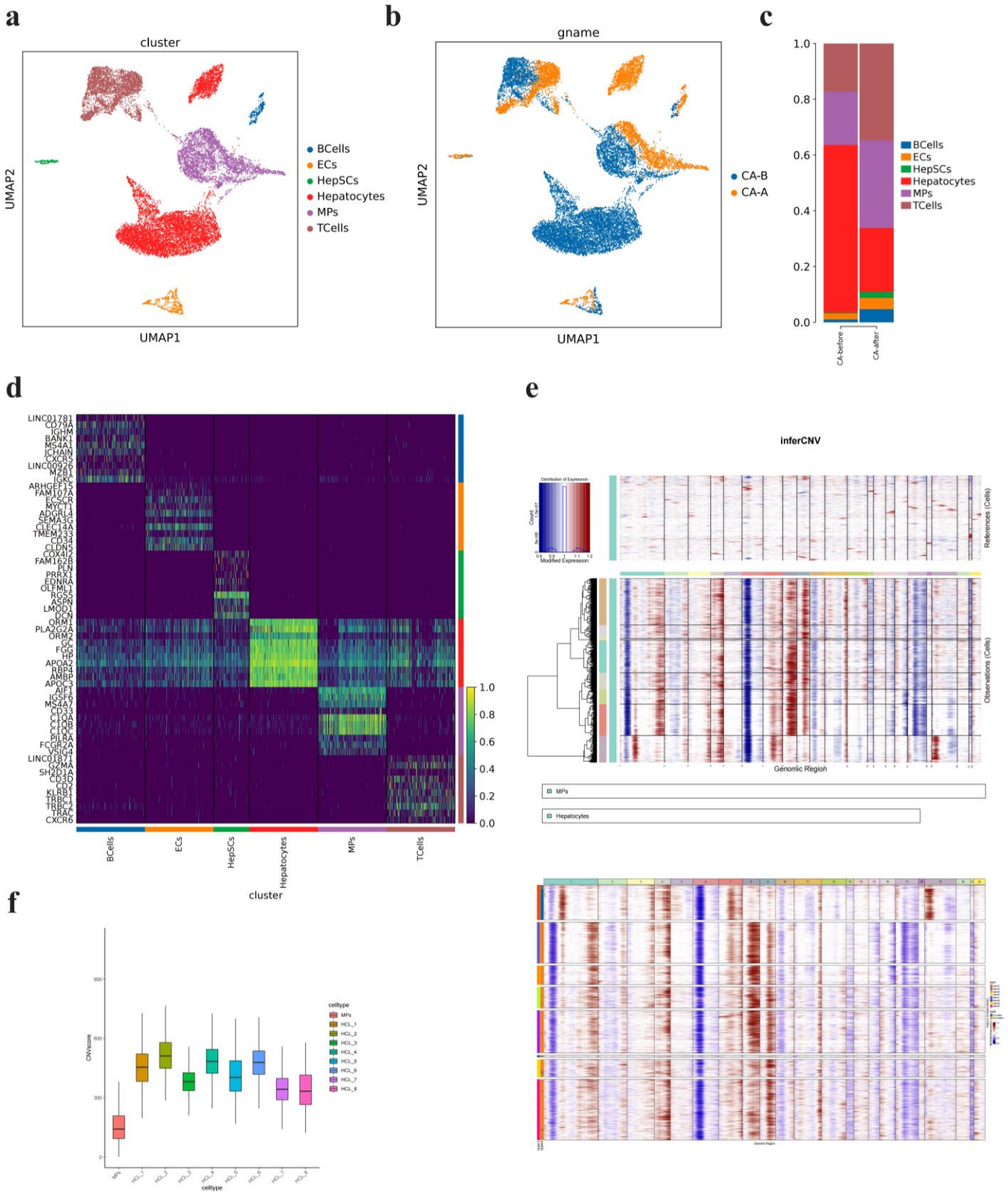


**Figure 2.** Global transcriptome landscape of hepatocellular carcinoma samples before and after drug administration.

a: A UMAP cell population map was formed by dimensionality reduction clustering, and a total of 6 cell types were obtained, including B cells, endothelial cells, hepatic stellate cells, hepatocytes, mononuclear macrophages and T cells. Different colors represent different cell types.

b: The distribution of various cell types before and after treatment. Blue represents before treatment and yellow represents after treatment.

c: Heat map of marker genes for each cell type.

d: Histogram of the percentages of each cell type before and after treatment.

e: Analysis of copy number variation (CNV) in hepatocytes using mononuclear macrophages as areference.

f: CNVscore.

## 3.2. Single-cell transcriptome profile on larger HCC mass

scRNA-Seg result were showed **Tables 1** and **2** on the major HCC mass before and after treatment. Naive cells were harvested from her HCC smaller mass (except the major mass) before and after major mass with UMIPIC therapy (**Figure 1a,b**). After multiple therapy to the major tumor mass, those untreated tumor masses were biopsied. Those cancer cell with lowest activity (<3%) were not qualified for SC-sequencing (**Figure 2c,d**).

**Table 1.** Summary of cell types and variations.

| Cell cluster | Cancer Before Therapy | Cancer After Therapy |
|---|---|---|
| B Cell | 124 | 262 |
| T Cells | 2118 | 1943 |
| ECs | 268 | 229 |
| HepSCs | 38 | 119 |
| Hepatocytes | 7362 | 1281 |
| MPs | 2339 | 1758 |

**Table 2.** Cell types and their specific markers.

| Label | Cell Type | Markers |
|---|---|---|
| Hepatocytes | Hepatocytes | ALB, APOB, APOA1, APOC3 |
| MPs | Mononuclear phagocytes | C1QC, MRC1, FCER1A, CD1C, VCAN, CD14 |
| TCells | T cells | CD2, CD3D, TRAC, TRBC2 |
| HepSCs | Hepatic stellate cells | ACTA2, RGS5, PDGFRB, TAGLN |
| ECs | Endothelial cells | CDH5, CLDN5, PECAM1, VWF |
| BCells | B cells | MS4A1, CD79A, CD79B |

## 3.3. Result of global transcriptome characteristics of HCC before and after drug administration

We obtained total of 17,841 RNA transcription profile with six cell populations by normalizing gene expression profiles, principal component analysis, and graph-based clustering methods (**Figure 2**), we annotated these cells into three major categories: Immune cells (T cells, B cells, and Mononuclear phagocytes), stromal cells (Hepatic stellate cells and endothelial cells), and Hepatocytes (**Figure 2b**).

scRNA-Seg was performed on two biopsied from untreated tumor samples before and after UMIPIC to largest tumor mass. Six cell populations were obtained by dimensionality reduction clustering (**Figure 2a**) based on labeling marker genes of

each cell: B cell, EC, Hepscs, hepatocytes, MP and T cells. Tumor copy number variation analysis (inferCNV) we used mononuclear macrophages as the baseline, it was found that significant copy number variation occurred in hepatocytes. For example, in the hepatocytes, prior treatment there were many insertions on chromosomes 1, 4, 7, 8, and 9, and a large number of fragment deletions on chromosomes 1, 6, 17, and 21. This finding is in agreement of the consensus that HCC are malignant based on significant insertions on chromosomes 1 and 19 (**Figure 2e**). Based on analysis of CNVscore of hepatocytes and MPs (reference cell), the malignant score of hepatocytes was relatively low (HCL_7) following the treatment at the major tumor mass (**Figure 2f**). Analysis of proportion of each cell types before and after treatment revealed a significant decrease in number of hepatocytes and an increase in parts of immune cells (**Figure 3c**).

### 3.4. Changes in tumor cells before and after drug administration

Tumor cells were further subdivided into 5 subclusters: cancer cell 1, 2, 4, and 5 were have huge reduction or nearly disappearing after treatment. While there comes a new tumor subset, i.e., cancercell 3 (**Figure 3a–c**). By comparing with tumor cell subclusters before treatment as a control, this new group of cells (group 3) have higher differentiation ability, angiogenesis and immune cell recruitment (**Figure 3g**). For cancercell 3, MT1E expression was upregulated. In addition, the RSS score was highest for the transcription factor HNF4A (**Figure 4e**), a member of the nuclear hormone receptor superfamily HNF, which plays a key role in the regulation of hepatocyte phenotypic differentiation. HNF4A is upstream of the transcriptional regulatory network and can interact with promoters and enhancers of various target genes.

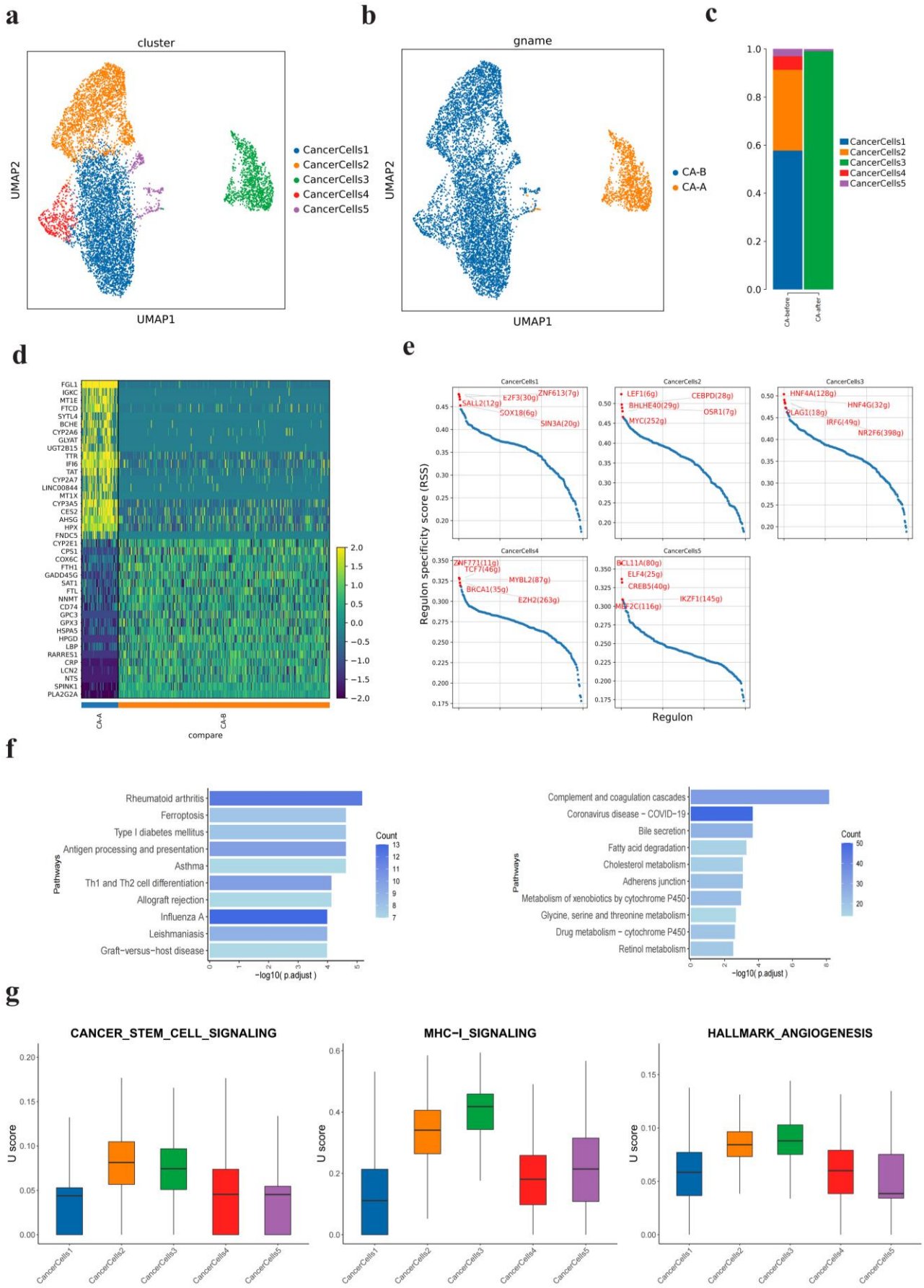


**Figure 3.** Changes of tumor cells before and after drug administration.

a: Subpopulations of tumor cells were subdivided, and UMAP cell population map was formed by dimensionality reduction clustering. A total of 5 tumor cell subpopulations were obtained, and different colors represented different subpopulations.

b: The distribution of various tumor cell subsets before and after treatment, with blue representing before and yellow representing after treatment.

c: Histogram of the proportion of each tumor cell before and after treatment.

d: Heat map of differential genes in tumor cells before and after treatment.

e: Display of TOP5 active transcription factors in each tumor cell subpopulation.

f: KEGG pathway enrichment analysis of differential genes in tumor cells before and after treatment (left panel shows down-regulated pathway, right panel shows up-regulated pathway).

g: Scores of MHC-I and angiogenesis related gene sets in each subpopulation of tumor cells.

## 3.5. Changes in immune cells before and after drug administration

T cell analysis: T cells were subdivided in analysis of changes in immune microenvironment in untreated tumor before and after the major mass treatment.

Six T-cell subclusters were obtained: CD8Teff, CD8Tem, Helper T, NK, Proliferating T, and Treg (**Figure 4a**). Proportions of NK cells and helper T cells were significantly increased (**Figure 4b**). In post treatment group, we found that 1, cytotoxicity-related genes of CD8 effector T cells and NK cells were upregulated (**Figure 4c**); 2, concurrently, CD8 effector T cells was also upregulated in terms of expression of tissue-resident T cell-related markers (21) (**Figure 4d**); 3, proportion of Helper T cells increased significantly; 4, marker genes of TH1 cells was upregulated (**Figure A1c**, See Appendix) and Th1 cells released a series of cytokines, including interferon γ (IFN-γ), interleukin-2 (IL-2) and tumor necrosis factor-β (TNF-β).

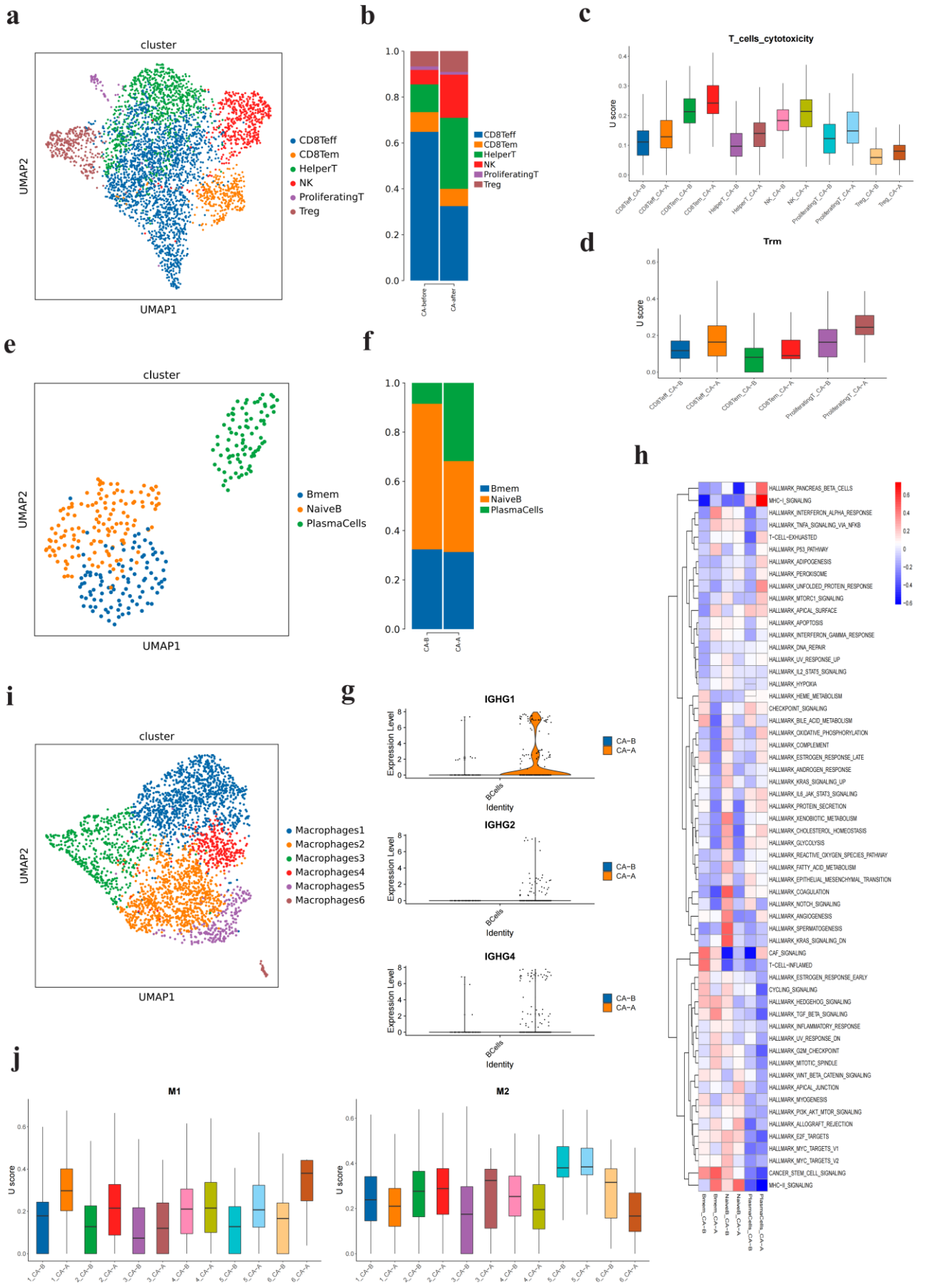


**Figure 4.** Changes of immune cells before and after drug administration.

a: Subpopulations of T cells were subdivided, and a UMAP cell population map was formed by dimensionality reduction clustering. A total of 6 T cell subpopulations were obtained, and different colors represented different subpopulations.

b: Histogram of the percentages of each T cell subsets before and after treatment.

c: Cytotoxicity related genes were used as the gene set to score various T cell subtypes before and after treatment.

d: marker genes of tissue-resident T cells were used as gene sets to score various T cell subtypes before and after treatment.

e: Subpopulations of B cells were subdivided, and a UMAP cell population map was formed by dimensionality reduction clustering. A total of three T cell subpopulations were obtained, and different colors represented different subpopulations.

f: Bar chart of the proportion of each B cell subsets before and after treatment.

G: Expression of the signature genes IGHG1, IGHG2 and IGHG4 of humoral immune response mediated by B cells before and after treatment in B cells.

h: Functional score of each subpopulation of B cells before and after treatment.

i: macrophages were subdivided into subgroups, and a UMAP cell group diagram was formed by dimensionality reduction clustering. A total of 5 subgroups were obtained, and different colors represent different subgroups.

j: macrophage subgroup was evaluated by using M1 and M2 macrophage marker genes as the gene set.

B cell analysis: three B cell subclusters were obtained: Bmem, Naive B cells and Plasma Cells (**Figure 4e**). The number of plasma cells increased after treatment (**Figure 4f**). Based on temporal trajectory analysis, all of B cells differentiated toward functional B cells after treatment (**Figure A1d**). In adaptive immunity, B cells express MHCI antigens, from Naive B cells to functional B cells and plasma cells. Naive B cells significantly upregulated MHC II signaling pathway-related genes, while plasma cells upregulated MHC I-related genes (**Figure 4h**).

Macrophage, monocytes, and cDCs were obtained by subdividing the MPs for further classification. 3 clusters were obtained (**Figure A1a**). Macrophages were further divided into six subclusters. Each cluster was scored by using marker genes of M1 and M2 as the gene set. The macrophages were found to show more M1 phenotype after treatment (**Figure 4j**) and M1 macrophages are anti-angiogenic which promotes chronic inflammation. It further confirmed by combining the TCGA database under the condition of low expression of MMP9, the survival rate was significantly improved ($P$ = 0.0087) (**Figure 5**). After treatment, the expression of MMP9 in macrophages was significantly down-regulated (**Figure 6f**).

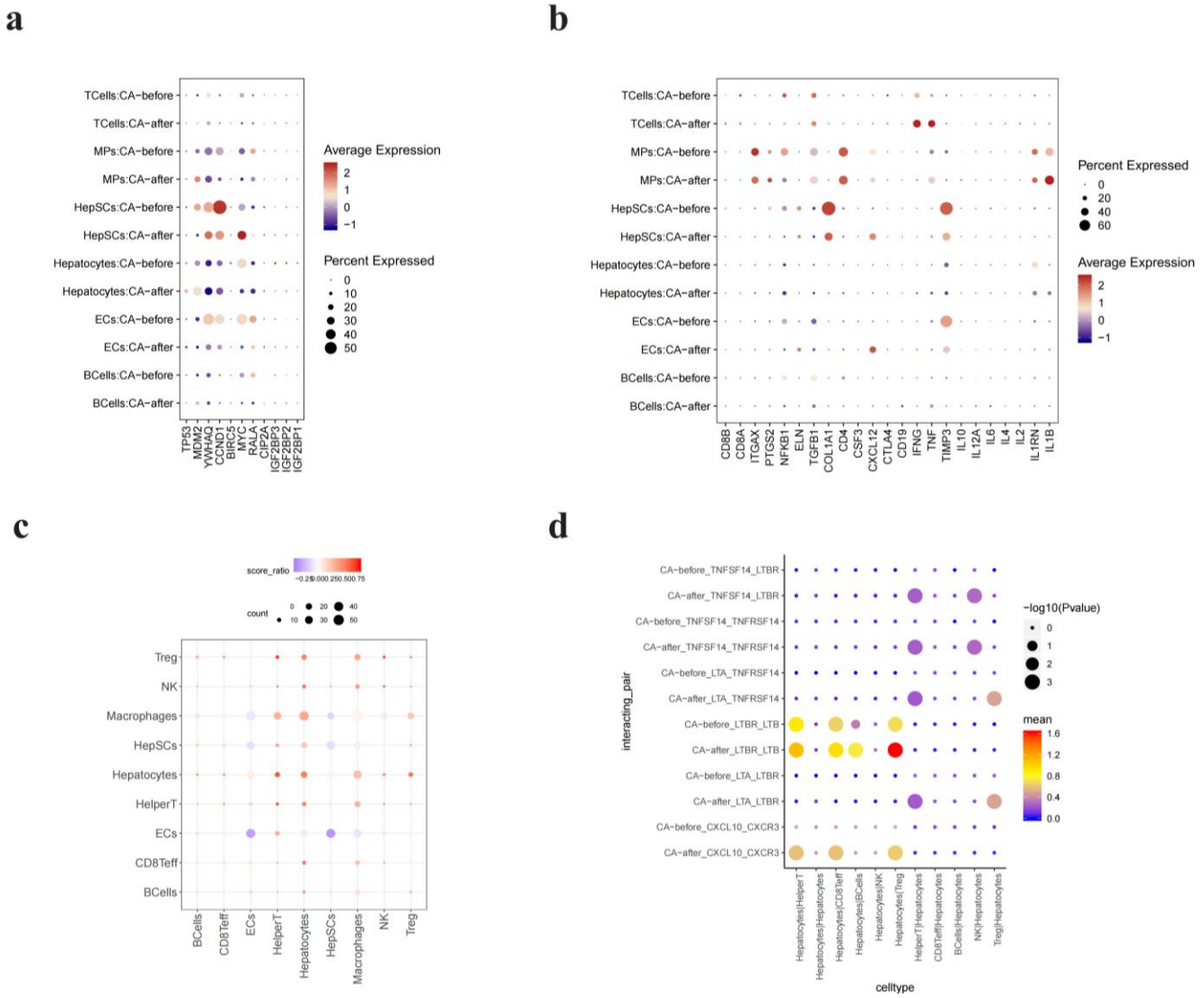


**Figure 5.** Cytokines and intercellular communication.

a: The expression of tumor factors in various types of cells before and after treatment. The redder the color, the stronger the gene expression intensity, and the larger the circle, the more cells expressing the gene.

b: Cytokine expression in various groups of cells before and after treatment. The redder the color, the stronger the gene expression intensity, and the larger the circle, the more cells expressing the gene.

c: Bubble diagram of intercellular interaction, the horizontal and vertical coordinates are the cell types interacting, bubble size represents the number of interactions (show the number of groups with a large number), bubble color represents the difference in the intensity of interaction between groups, red represents the intensity after treatment, blue represents the intensity before treatment.

d: Cytokine interactions that play a key role in the development of cirrhosis are shown. The circle size indicates the significance of the interaction, and the redder the color, the stronger the interaction strength.

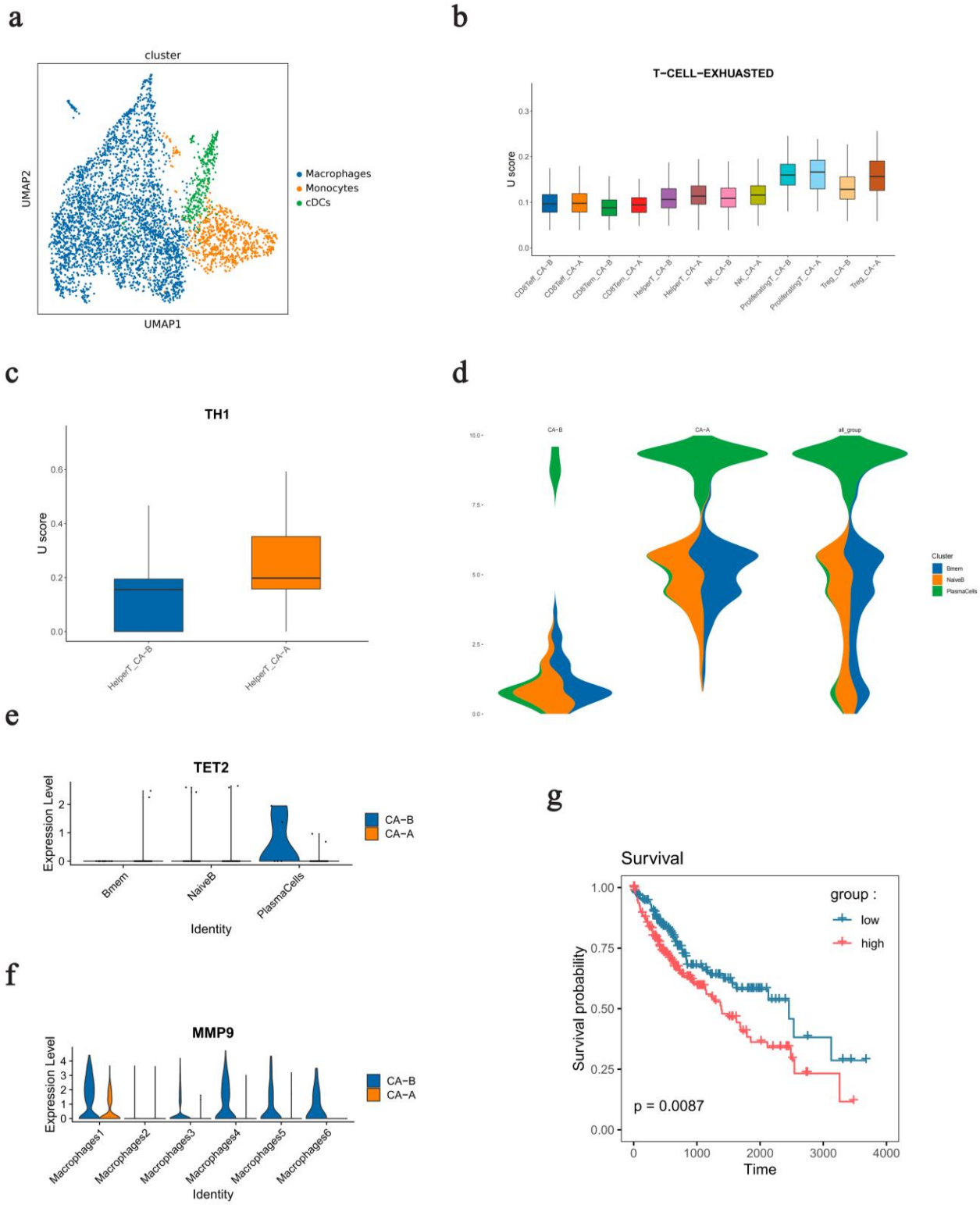


**Figure 6.** Cytokines and intercellular communication.

a: MPs were subdivided into subpopulations, and a UMAP cell population map was formed by dimensionality reduction clustering. A total of 6 T cell subpopulations were obtained, and different colors represented different subpopulation.

b: marker gene of TH1 cells was used as gene set to score Helper T cells before and after treatment.

c: T cell depletion related genes were used as the gene set to score various T cell

subtypes before and after treatment.

d: Temporal trajectory analysis of B cells.

e: Expression of TET2 gene in B cells before and after treatment.

f: Expression of MMP9 gene in each subgroup of Macrophages after treatment.

g: To evaluate the correlation between high and low expression of MMP9 and the prognosis of HCC patients according to the information of TCGA database.

### 3.6. Cytokines and intercellular communication

The expression of oncogene MYC was down regulated in hepatocytes (tumor cells) after treatment (**Figure 5a**). In contrast, T cells overall showed up-regulation of effector markers IFNG and TNF (**Figure 5b**). By analyzing cell-cell communication, the interaction between hepatocytes (tumor cells) and immune cells was enhanced after treatment (**Figure 5c**). The chemokine CXCR3 was expressed on activated CD4, CD8T cells and NK cells. This plays an important role in the migratory behavior and cell interactions of T cells in both lymphoid compartments and peripheral tissues.

## 4. Discussion

Fewer drugs and treatment strategies are available for progressed or later stages HCC. Local and novel treatments, i.e., immune therapies, are necessary for these patients [23,24]. Localized intervention can kill tumor cells on site of tumor, concurrently induce immune reactions [7–9]. This kind of option has achieved some success and showed promising development [25.] Hapten combined with chemotherapeutic drugs has been successfully injected into the tumor to treat liver cancer. [6,7,25] All immunity reactions are related to the abscopal effect [26–30]. With scRNA-seq, we investigated all the changes at the molecular level for B and T cells on untreated tumor in nearby treated major tumor mass before and after intra-tumor injection with chemotherapeutic drugs plus hapten.

Clinical benefits were observed and obvious for this treatment such like patient's quality of life and the patient's feelings about everything changed to better pre-treatment more than 13 months ago. After multiple injections of UMIPIC, biopsies were taken again from non-treated tumor masses, the tumor cells with the lowest activity were less than 3%, and these cells lost quality of cell activity (**Figure 1c,d**) it indicated therapy was effective. CTC were detected through the course of treatment but showed a decreasing tread from 5/3 mL before treatment to 3/3 mL one week later and 2/3 mL two weeks later respectively (**Figure 1f**,**g**). It probably indicates that cancer cells are under control and not increased number of cancer cells released to circulation.

After the first treatment, the changes of the abnormal prothrombin (AP) from 19,184 ng/mL to 32,048 ng/mL in 102 days, it indicated AP released more than earlier since tumor death by UMIPIC. AP is a diagnostic maker for AFP-negative hepatocellular carcinoma, and it may reflect the degree of natural tumor progression as well as AFP. After 4 months AP return to 304 ng/mL lower than earlier. The expression of prothrombin coding gene F2 was up-regulated. The expression of the code gene VKORC was upregulated, as was the expression of the gene set associated with vitamin K metabolism, but clinical abnormal prothrombin remains high,

presumably to be verified at the genomic level (**Figure 7**). Prothrombin, also known as a coagulation factor II, is synthesized in liver tissue in a vitamin K-dependent manner [27]. Previous studies have shown that abnormal γ-carboxylase results from loss of normal enzyme gene expression or defective gene expression [29,30]. It indicated that the treatment is effective to control tumor growth.

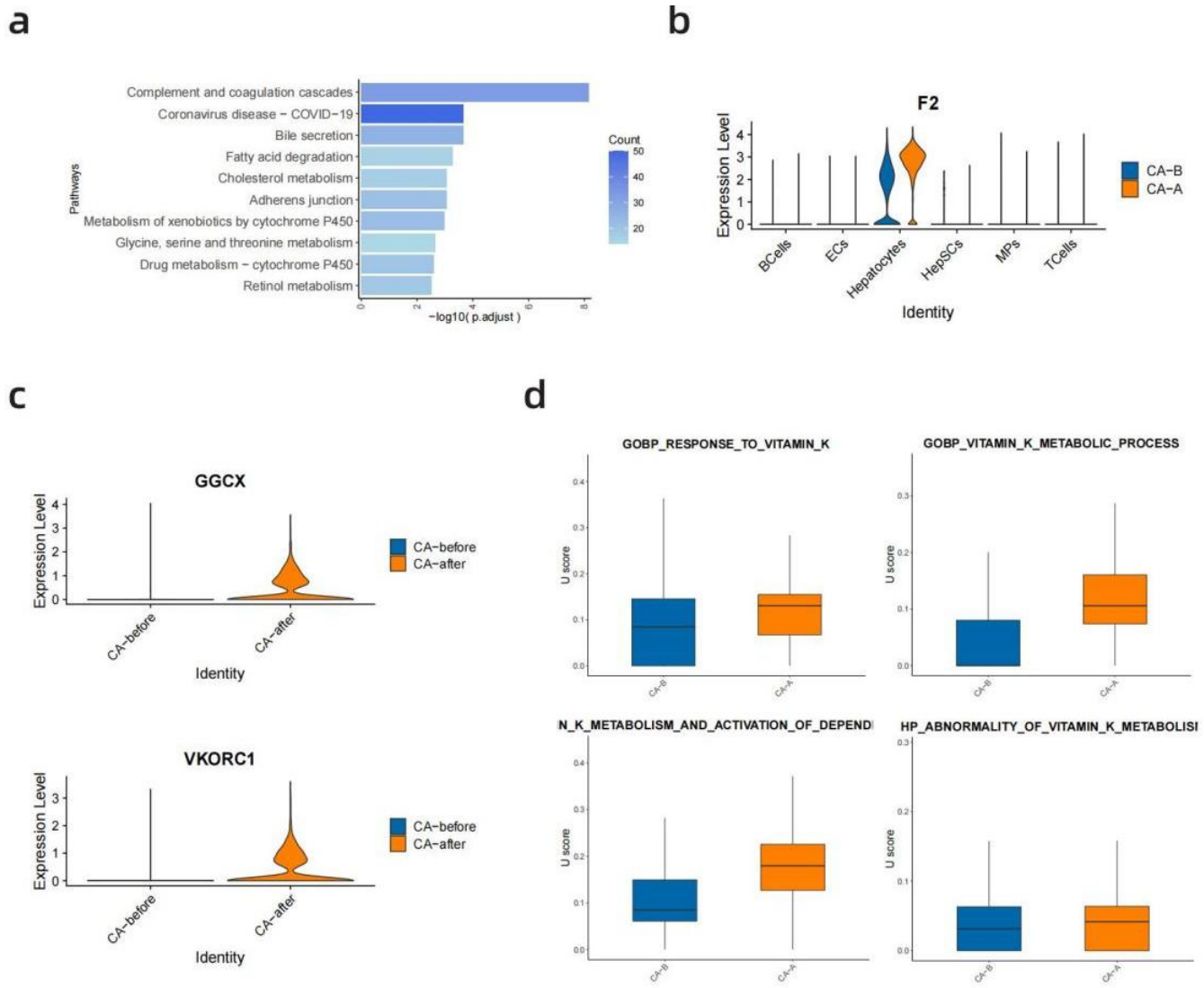


**Figure 7.** Analysis abnormal high prothrombin.

a. KEGG pathway enrichment analysis was performed on differential genes in hepatocytes before and after treatment. The enrichment analysis of KEGG pathway was conducted for the DEGs of hepatocytes before and after treatment, and the up-regulated genes were significantly enriched to the pathway of complement and coagulation cascade

b. Expression of prothrombin encoding gene F2 in various types of cells before and after treatment Treatment

c. Expression of γ-glutamyltransferase (GGT) encoding gene GGCX and vitamin K epoxide reductase complex 1 encoding gene VKORC1 in hepatocytes before and after treatment (Expression of GGCX) encoding gene GGCX and vitamin K epoxide

reductase complex, subunit 1 encoding gene VKORC1 in hepatocytes before and after treatment

d: Expression of GOBP_RESPONSE_TO_VITAMIN_K gene set, vitamin K metabolism related gene set, vitamin K metabolism and related protein activated gene set, vitamin K abnormal metabolism related gene set in hepatocytes before and after treatment set, GOBP_VITAMIN_K_METABOLIC_PROCESS gene set, wp_vitamin_k_metabolism_and_activation_of_dependent_proteins gene set, and hp_abnormality_of_vitamin_k_metabolism gene set in hepatocytes before and after treatment.

In this study, six cell populations were classified by dimensionality reduction clustering (**Figure 2a**), These cell types were annotated according to marker genes of each cell (**Figure 2c**): B Cell, ECs, Hepscs, Hepatocytes, MPs, and T cells respectively. The hepatocytes were identified as malignant based on CNVscore of hepatocytes and MPs (reference cell) (**Figure 2e**). The malignant degree of hepatocytes was relatively low after treatment (**Figure 2f**). An increase of the proportion of immune cells have confirmed the local injection to the major mass is effective and cause response from untreated tumor cell from other smaller masses (**Figure 2c**) [7–9]. The immune cells are recruited in large numbers due to hapten-modified tumor-associated antigens to stimulate the body's immune system and reacted to the neo tumor antigens.

Further comparison of untreated tumor cell subclusters before and after major mass treatment, cancer cell 3 had higher differentiation ability (**Figure 3g**). After analyzing of the differential genes of cancer cell 3 and cancer cell 1, 2, 4, and 5, we found that the tumor suppressor gene HAO2 [22] and metallothionein coding genes MT1E, MT1M, and MT1G were upregulated (**Figure 3d**). The RSS score was highest for the transcription factor HNF4A (**Figure 3e**). The coding genes of metallothionein family have different functions. MT1M and MT1E have been reported to suppress hepatocellular carcinoma cells [23,24]. A member of the nuclear hormone receptor superfamily (HNF) plays a key role in the regulation of hepatocyte phenotypic differentiation. HNF4A is upstream of the transcriptional regulatory network and can interact with promoters and enhancers of various target genes. HNF4A is usually highly expressed in normal hepatocytes but poorly expressed in HCC. However, when it is re-expressed, it can restore the hepatocyte phenotype of poorly differentiated HCC cells [28,30].

It is speculated that after drug plus hapten local injection treatment, due to the increased activity of HNF4A, the methylation levels of MT1E and MT1M promoters are upregulated, hence, tumor suppressor function of HNF4A is gradually restored. In Cancer cell 3, the expression of FGL1 is significantly increased. FGL1 is mainly secreted by hepatocytes in the liver, which is the product of hepatocyte regeneration and is involved in hepatocyte mitosis and liver energy utilization. Studies have shown that FGL1 is highly expressed in normal hepatocytes but down-regulated in hepatocellular carcinoma [31].

Down-regulation of the iron death pathway was also identified in functional enrichment analysis of differential genes in tumor cells before and after treatment (**Figure 3f**). Synaptotagmin-like protein 4 (SYTL4) is also upregulated in cancer cell 3. SYTL4 is a chemotherapeutic resistance gene [28]. Some of chemotherapeutic

drugs depend on the stability of microtubules in cells. These findings provide new ideas for guiding the combination drugs uses in the near future.

Previous studies have shown that natural killer (NK) cells and a cluster of differentiation 8 (CD8) cells are greatly reduced in liver tumor tissue samples [28] their function is also greatly inhibited with the development of tumors [31–33]. In this study, T cell subclusters were first subdivided in analyzing changes in the immune microenvironment in the untreated tumor in contrast to the major tumor with and without treatment. A total of 6 cell subclusters were obtained, which were CD8 Teff, CD8 Tem, Helper T, NK, Proliferating T, and Treg (**Figure 4a**). The percentages of NK cells and Helper T cells were significantly increased (**Figure 4b**). The cytotoxicity related genes were used as gene sets to score the T cell subclusters. We found that the cytotoxicity-related genes of CD8 effector T cells and NK cells were upregulated following treatment (**Figure 4c**). B cell-mediated humoral immune response marker genes IGHG1, IGHG2, IGHG4 were all upregulated (**Figure 4g**) [25]. Similarly, CD8 effector T cells upregulated the expression of tissue-resident T cell-related markers (**Figure 4d**). These changes will co-exert immune effects with T cells. In addition, we have found that TET2, an important epigenetic regulatory enzyme in B lymphocytes was down regulated after treatment [26].

After the subdividing B cells, three cell subclusters derived: Bmem, Naive B cells and Plasma Cells (**Figure 4e**). After treatment, number of plasma cells increased (**Figure 4f**). The signature genes of humoral immune response mediated by B cells, immunoglobulin heavy chain constant gamma 1 (IGHG1), IGHG2, and IGHG, were all upregulated (**Figure 4g**) [34]. Increasing of infiltration of plasma cells is a reflection of high-level immunity, which is one of the predictors of good prognosis [34]. According to temporal trajectory analysis, B cells all differentiated toward functional B cells after treatment (**Figure 71d**) and played an immune role. In adaptive immunity, B cells express histocompatibility complex I (MHC I) antigens, from Naive B cells to functional B cells and plasma cells. It mediates the interaction with T cells and is also involved in antigen presentation by B cells as helper T cells. After treatment with larger tumor mass, both Bmem and Naive B cells significantly upregulated MHC II signaling pathway-related genes. While plasma cells upregulated MHC I-related genes (**Figure 4h**), which may co-exert immune effects with T cells. In addition, studies have showed that methylcytidine dioxygenase 2 (TET2) was downregulated. TET2 is an important epigenetic regulatory enzyme in B lymphocytes, which promotes the production of regulatory B cells and thus promotes tumor progression [27]. The downregulation of TET2 expression after drug treatment (**Figure 71e**) is conducive to the prognosis of patients. It indicates that B cell is involved in autologous tumor immunity reaction by the hapten-modified tumor antigen and also reflects the abscopal effect at the molecular level of gene regulation.

The macrophage cells were further subdivided into 6 clusters were obtained (**Figure 4i**). Each cluster was scored by using marker genes of M1 and M2 as the gene set. Data shows that macrophages possess more M1 phenotype after treatment (**Figure 4j**). M1 macrophages have anti-angiogenesis function. It promotes chronic inflammation and inhibits tumor growth [34]. Reported research data have shown that the high expression of matrix metalloproteinase-9 (MMP9) in tumor-associated macrophages can promote the progression of HCC by inducing the migration,

invasion, and angiogenesis. These are indicators of poor prognosis [24]. It has been confirmed by combining The Cancer Genome Atlas (TCGA) database that lower expression of MMP9, the survival rate was significantly improved ($P$ = 0.0087) (**Figure 71g**). Expression of MMP9 in macrophages after treatment was significantly down-regulated (**Figure 71f**), which was beneficial for patient prognosis.

In addition, the expression of tumor necrosis factor family related interactions was upregulated. These include TNFSF14, lymphotoxin LTA, and LTB, we know these members promoted anti-tumor immunity (**Figure 5d**).

Expression of oncogene myelocytomatosis (MYC) was downregulated after treatment in hepatocytes (tumor cells) (**Figure 6a**). In contrast, T cells overall showed up-regulation of effector markers interferon gamma (IFNG) and TNF (**Figure 4b**), leading to the sustained killing of tumor cells. Combined with clinical efficacy with tumor stable and KPS score goes higher, the T cells is playing an important role in control untreated tumor growth which is an abscopal effect.

From the analysis of the cell-cell communication, we found that the interaction between hepatocytes (tumor cells) and immune cells was enhanced after treatment (**Figure 6c**). The chemokine receptor 3 (CXCR3) was expressed on activated CD4, CD8, T cells and NK cells (**Figure 3d**). CXCR3 plays an important role in cell migration and cell interaction of T cells in the lymphoid compartment and peripheral tissues and make immune cells ready to activate the CD8+ effector T cells in sensitized state. CXCR3 can bind the chemokine ligand 10 (CXCL10) to induce the migration of activated T cells to the sites of infection and inflammation, including CD4+TH1 cells and CTL+CD8_T cells, then stimulate the secretion of IFNγ [32]. In addition, the expression of tumor necrosis factor family-related interactions was upregulated (**Figure 6d**). These include TNFSF14, lymphotoxin-alpha (LTA) and lymphotoxin-beta (LTB), which promoted anti-tumor immunity.

In short, to prove that the abscopal is a complex immunity reaction that not only involves B cell activity but also involves T cell activity with multiple genes participating at the molecular level. It can be induced through UMIPIC not radiation therapy. This plays an important role in the modification of associated tumor antigens (ATAs) to improve neu ATAs. Finally, further detailed studies with more multifocal tumor of HCC cases for hapten-enhanced intra-tumoral injections are required to develop a comprehensive understanding of the full mechanism of therapeutic potential and new treatment paradigms.

**Author contributions:** Conceptualization, BY; methodology, FG; software, PJ; validation, PZ and GZ; formal analysis, BY; investigation, FG; resources, PJ; data curation, JZ; writing—original draft preparation, BY; writing—review and editing, BY; visualization, BY; supervision, BY; project administration, GZ. All authors have read and agreed to the published version of the manuscript.

**Acknowledgments:** The authors appreciate valuable scientific advice from Shi Yang, Department of Pathology and Laboratory Medicine, Boston University Chobanian & Avedisian School of Medicine, Boston, Massachusetts USA in preparing of this manuscript. This study was sponsored by TaiMei Baofa Cancer hospital (Dongping, Shandong Province, China, 271500).

**Data availability statement:** The data that support the findings of this study are available from [third party name] but restrictions apply to the availability of these data, which were used under license for the current study, and so are not publicly available. Data are however available from the authors upon reasonable request and with writing permission of [third party name] to Baofa Yu.

**Conflict of interest:** The authors declare no conflict of interest.

## References

1. Xia C, Dong X, Li H, et al. Cancer statistics in China and United States, 2022: profiles, trends, and determinants. Chinese Medical Journal. 2022; 135(5): 584-590. doi: 10.1097/cm9.0000000000002108
2. Dong L, Peng L, Ma L, et al. Heterogeneous immunogenomic features and distinct escape mechanisms in multifocal hepatocellular carcinoma. Journal of Hepatology. 2020; 72(5): 896-908. doi: 10.1016/j.jhep.2019.12.014
3. Liu CY, Chen KF, Chen PJ. Treatment of Liver Cancer. Cold Spring Harbor Perspectives in Medicine. 2015; 5(9): a021535. doi: 10.1101/cshperspect.a021535
4. Xu F, Jin T, Zhu Y, et al. Immune checkpoint therapy in liver cancer. Journal of Experimental & Clinical Cancer Research. 2018; 37(1). doi: 10.1186/s13046-018-0777-4
5. Yu B, Lu Y, Gao F, et al. Hapten-enhanced therapeutic effect in advanced stages of lung cancer by ultra-minimum incision personalized intratumoral chemoimmunotherapy therapy. Lung Cancer: Targets and Therapy. 2015; 1. doi: 10.2147/lctt.s70679
6. Yu B, Gao F, Jing P, et al. Hapten-enhanced overall survival time in advanced hepatocellular carcinoma by ultro-minimum incision personalized intratumoral chemoimmunotherapy. Journal of Hepatocellular Carcinoma. 2015; 57. doi: 10.2147/jhc.s80756
7. Gross BP, Wongrakpanich A, Francis MB, et al. A Therapeutic Microparticle-Based Tumor Lysate Vaccine Reduces Spontaneous Metastases in Murine Breast Cancer. The AAPS Journal. 2014; 16(6): 1194-1203. doi: 10.1208/s12248-014-9662-z
8. Diao L, Liu M. Rethinking Antigen Source: Cancer Vaccines Based on Whole Tumor Cell/tissue Lysate or Whole Tumor Cell. Advanced Science. 2023; 10(22). doi: 10.1002/advs.202300121
9. Max S, Peter G, Christoph S, et al. Tumor cell lysate-pulsed human dendritic cells induce a T-cell response against pancreatic carcinoma cells: an in vitro model for the assessment of tumor vaccines. Cancer Res. 2001; 61(17): 6445-50.
10. Ziegenhain C, Vieth B, Parekh S, et al. Comparative Analysis of Single-Cell RNA Sequencing Methods. Molecular Cell. 2017; 65(4): 631-643. doi: 10.1016/j.molcel.2017.01.023
11. Ma L, Hernandez MO, Zhao Y, et al. Tumor Cell Biodiversity Drives Microenvironmental Reprogramming in Liver Cancer. Cancer Cell. 2019; 36(4): 418-430. doi: 10.1016/j.ccell.2019.08.007
12. Kaminski JM, Shinohara E, Summers JB, et al. The controversial abscopal effect. Cancer Treatment Reviews. 2005; 31(3): 159-172. doi: 10.1016/j.ctrv.2005.03.004
13. Abuodeh Y, Venkat P, Kim S. Systematic review of case reports on the abscopal effect. Current Problems in Cancer. 2016; 40(1): 25-37. doi: 10.1016/j.currproblcancer.2015.10.001
14. Yu B, Fu Q, Han Y, et al. An Acute Inflammation with Special Expression of CD11 & CD4 Produces Abscopal Effect by Intramoral Injection Chemotherapy Drug with Hapten in Animal Model. Journal of Immunological Sciences. 2022; 6(3): 1-9. doi: 10.29245/2578-3009/2022/3.1236
15. Huisse MG, Leclercq M, Belghiti J, et al. Mechanism of the abnormal vitamin K-dependent gamma-carboxylation process in human hepatocellular carcinomas. Cancer. 1994; 74(5): 1533-1541. doi: 10.1002/1097-0142(19940901)74:5<1533:aid-cncr2820740507>3.0.co;2-v
16. Ge F, Zhang H, Wang DD, et al. Enhanced detection and comprehensivein situphenotypic characterization of circulating and disseminated heteroploid epithelial and glioma tumor cells. Oncotarget. 2015; 6(29): 27049-27064. doi: 10.18632/oncotarget.4819
17. Lin PP, Gires O, Wang DD, et al. Comprehensive in situ co-detection of aneuploid circulating endothelial and tumor cells. Scientific Reports. 2017; 7(1). doi: 10.1038/s41598-017-10763-7
18. Wolf FA, Angerer P, Theis FJ. SCANPY: large-scale single-cell gene expression data analysis. Genome Biology. 2018;

19(1). doi: 10.1186/s13059-017-1382-0
19. Korsunsky I, Millard N, Fan J, et al. Fast, sensitive and accurate integration of single-cell data with Harmony. Nature Methods. 2019; 16(12): 1289-1296. doi: 10.1038/s41592-019-0619-0
20. Dong R, Yang R, Zhan Y, et al. Single-Cell Characterization of Malignant Phenotypes and Developmental Trajectories of Adrenal Neuroblastoma. Cancer Cell. 2020; 38(5): 716-733. doi: 10.1016/j.ccell.2020.08.014
21. Andreatta M, Carmona SJ. UCell: Robust and scalable single-cell gene signature scoring. Computational and Structural Biotechnology Journal. 2021; 19: 3796-3798. doi: 10.1016/j.csbj.2021.06.043
22. Qian W, Zhao M, Wang R, et al. Fibrinogen-like protein 1 (FGL1): the next immune checkpoint target. Journal of Hematology & Oncology. 2021; 14(1). doi: 10.1186/s13045-021-01161-8
23. Liu Q, Lu F, Chen Z. Identification of MT1E as a novel tumor suppressor in hepatocellular carcinoma. Pathology—Research and Practice. 2020; 216(11): 153213. doi: 10.1016/j.prp.2020.153213
24. Lu Z, Liu R, Wang Y, et al. Ten-eleven translocation-2 inactivation restrains IL-10-producing regulatory B cells to enable antitumor immunity in hepatocellular carcinoma. Hepatology. 2022. doi: 10.1002/hep.32442
25. Inagaki Y, Tang W, Makuuchi M, et al. Clinical and molecular insights into the hepatocellular carcinoma tumour marker des-γ-carboxyprothrombin. Liver Int. 2011; 31(1): 22-35. doi: 10.1111/j.1478-3231.2010.02348.x
26. Liu XY, Jiang W, Ma D, et al. SYTL4 downregulates microtubule stability and confers paclitaxel resistance in triple-negative breast cancer. Theranostics. 2020; 10(24): 10940-10956. doi: 10.7150/thno.45207
27. Sun X, Niu X, Chen R, et al. Metallothionein-1G facilitates sorafenib resistance through inhibition of ferroptosis. Hepatology. 2016; 64(2): 488-500. doi: 10.1002/hep.28574
28. Zhang L, Yu X, Zheng L, et al. Lineage tracking reveals dynamic relationships of T cells in colorectal cancer. Nature. 2018; 564(7735): 268-272. doi: 10.1038/s41586-018-0694-x
29. Terrén I, Orrantia A, Vitallé J, et al. NK Cell Metabolism and Tumor Microenvironment. Frontiers in Immunology. 2019; 10. doi: 10.3389/fimmu.2019.02278
30. Zheng C, Zheng L, Yoo JK, et al. Landscape of Infiltrating T Cells in Liver Cancer Revealed by Single-Cell Sequencing. Cell. 2017; 169(7): 1342-1356. doi: 10.1016/j.cell.2017.05.035
31. Zhang S, Liu Z, Wu D, et al. Single-Cell RNA-Seq Analysis Reveals Microenvironmental Infiltration of Plasma Cells and Hepatocytic Prognostic Markers in HCC With Cirrhosis. Frontiers in Oncology. 2020; 10. doi: 10.3389/fonc.2020.596318
32. Groom JR, Luster AD. CXCR3 in T cell function. Experimental Cell Research. 2011; 317(5): 620-631. doi: 10.1016/j.yexcr.2010.12.017
33. Cheng Z, He Z, Cai Y, et al. Conversion of hepatoma cells to hepatocyte-like cells by defined hepatocyte nuclear factors. Cell Research. 2018; 29(2): 124-135. doi: 10.1038/s41422-018-0111-x
34. Xing T. Molecular and immunophenotyping of liver cancer and the research progress of immune combined targeted therapy. Chinese Journal of Hepatobiliary Surgery. 2021; 27(7): 4.

## Appendix

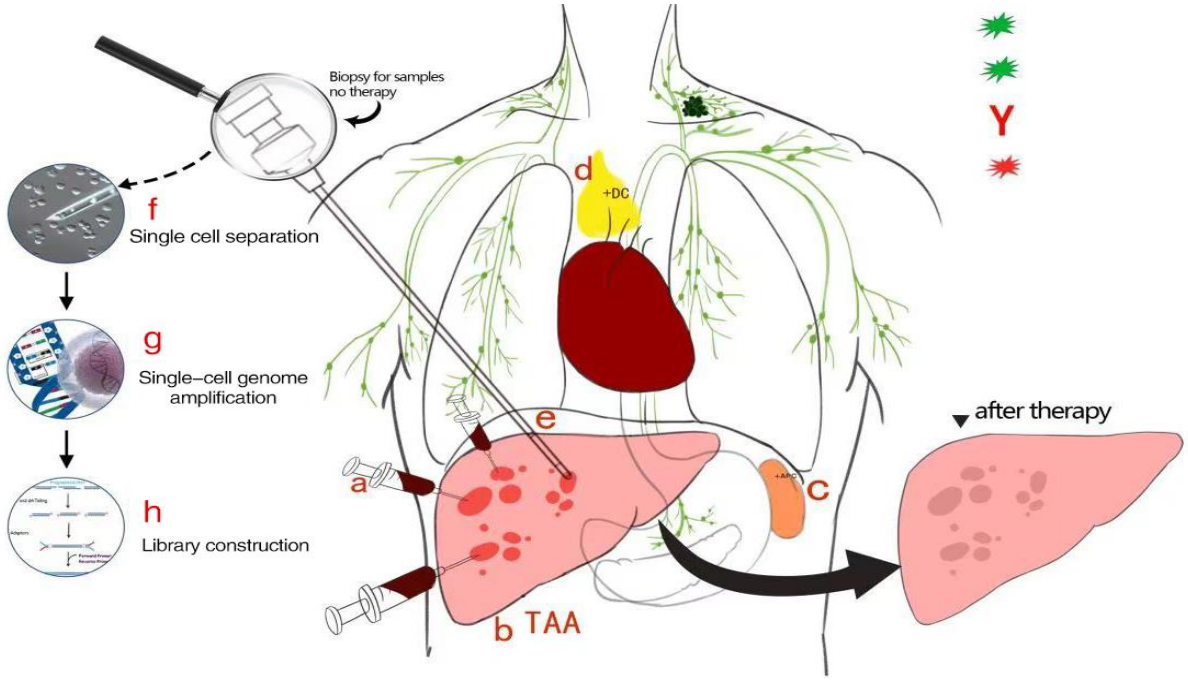


**Figure A1.** Graphic abstract of schematic diagram of single-cell sequencing process for liver cancer.

a: Syringe for injection with chemotherapy drug plus hapten into primary tumor in the scope of big tumor area, cause the tumor cell death, necrosis with inflammation, there is an haptenization with the tumor antigen released from death tumor cells be strong tumor antigens as neu tumor antigens (TAA) while DC cell capture the neu tumor antigens for antigen presentation process.

b: After DC cell capture the neutumor antigens for antigen presentation process, the immune system of patient body produce the related tumor autologous antibodies (iTAA).

c: The antibodies and cytokines may produce from lymph nodes or immune system and can circulate in the blood to find the tumor where the metastasis cell was, like metastasis in the supraclavicular lymph node, and bind the antigen on the tumor cell membrane or nuclear of metastasis to make the changes at molecular level in sentinel lymph node as a window for watching.

d: Thymus and spleen involved in the immune reaction to produce cytokines and antibodies from immune system and can circulate in the blood to find the tumor where the metastasis cell was, like metastasis in the lymph node, and bind the antigen on the tumor cell membrane or nuclear of metastasis to make the changes at molecular level in sentinel lymph node as a window for watching.

e: Using the biopsy needle to take a small part of untreated tumor tissue before and after intratumoral injection to the primary tumor near by the untreated tumor in order to evaluate the changes at molecular level.

f: After took the tumor tissue, immediately brought to the laboratory and tissue disassociation for cell separation.

g: Analysis of single cell genome application profile.

h: Genome library construction.